140

Superconductivity in twisted bilayer WSe₂

CNF Project Number: 263318

Principal Investigator(s): Jie Shan, Kin Fai Mak User(s): Zhongdong Han, Yiyu Xia, Yichi Zhang

Affiliation(s): Laboratory of Atomic and Solid State Physics, School of Applied and Engineering Physics; Cornell University

Primary Source(s) of Research Funding: DOE, NSF, AFOSR, Moore Foundation

Contact: jie.shan@cornell.edu, kinfai.mak@cornell.edu, zh352@cornell.edu, yx579@cornell.edu, yz2662@cornell.edu Website: https://sites.google.com/site/makshangroup/

Primary CNF Tools Used: Zeiss Supra SEM, Nabity Nanometer Pattern Generator System (NPGS), Angstrom E-Beam Evaporator, SC4500 Odd/Even-Hour Evaporator, Oxford 81/82 RIE, YES Asher, Autostep i-line Stepper, Hamatech Wafer Processor Develop, Heidelberg Mask Writer - DWL2000, Photolithography Spinners, Dicing Saw - DISCO

Abstract:

Semiconductor moiré materials have emerged as a highly tunable platform for simulating the Hubbard model [1,2], which is believed to capture the essential physics of high-temperature superconductors [3]. However, the experimental evidence for superconductivity in these systems remains elusive. Here, we report the observation of robust superconductivity in twisted bilayers WSe₂. Our results reveal its unconventional nature rooted in strong electron correlations.

Summary of Research:

The Hubbard model [4], a simplest model describing interacting electrons on a lattice, provides profound insights into the physics of strongly correlated particles. Tuning the effective interaction strength to the moderate correlation regime is expected to stabilize a variety of exotic phases near the Mott transition. A well-known example is the idea that doping a Mott insulator captures the essential physics underlying high transition temperature (Tc) superconductors [5,6]. Developing a controllable platform to simulate Hubbard model physics and high-Tc phenomenology is highly desirable, as it could offer new perspectives on the high-Tc problem and guide the design of next-generation high-temperature superconductors.

In this study, we investigate the electrical transport properties of a 3.65° twisted bilayer WSe2 (tWSe2) device with tunable carrier density n and out-of-plane electric field E. Our measurements establish the electrostatic phase diagram for tWSe2 at moderate correlation regime. At half-band filling, a Mott insulator is observed, with its correlation strength effectively controlled by the electric field. Upon approaching the metal-insulator transition near zero E field—where the hopping amplitude t becomes comparable with the onsite interaction U—we observe robust superconductivity.

The optimal superconducting temperature is about 200 mK, corresponding to about 1-2% of the effective Fermi temperature. This ratio is comparable to that of high-temperature cuprate superconductors and suggests strong pairing.

Figure 1 shows the device schematics (a) and its optical image (b). The encapsulated twisted bilayer WSe2 is directly transferred onto prepatterned Pt electrodes. The dual-gated geometry enables independent tuning of n and E. Additional contact and split gates, deposited atop the full stack, are implemented to achieve low contact resistances and eliminate unwanted parallel conduction channels. The Hall-bar geometry is defined by all four gates, including the top, bottom, contact and splitting gates. Electrical transport measurements are performed in a dilution refrigerator, equipped with low-temperature resistor-capacitor and radiofrequency filters mounted on the mixing chamber plate to attenuate electrical noise from about 65 kHz to tens of gigahertz. Low-frequency (5.777 Hz) lock-in techniques are employed to measure sample resistance using a small excitation current (<10 nA) to avoid sample heating.

Figure 2 shows the longitudinal resistance R measured as a function of moiré filling factor v and E (a) and a zoom-in phase diagram near half-band filling (v=1) and zero E field (b). In the electrostatic phase diagram, the layer-shared (inner) and layer-polarized (outer) regions are delineated by dashed lines. In the layer-shared region, the van Hove singularity (vHS), characterized by a diverging density of states (DOS), is identified as a high-resistance feature traced by the red curve. Overall, the phase diagram aligns well with the single-particle expectation, except for the correlated insulating states observed at commensurate fillings v=1/4,1/3,1. Notably, at v=1, a robust zero-resistance phase emerges at the verge of the correlated insulator near zero E field.

Cornell NanoScale Facility

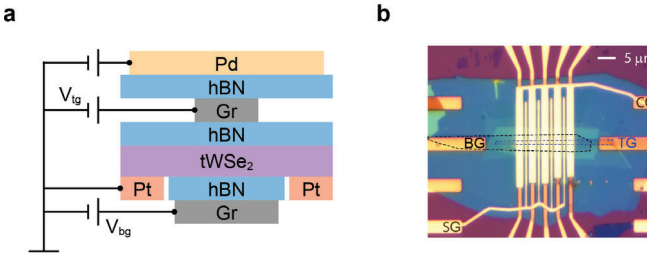


Figure 1: a, Schematic of the device structure. b, Optical microscope image of a 3.65° tWSe2 device. Scale bar is 4 µm.

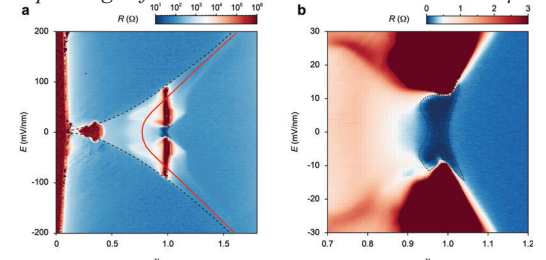


Figure 2: a, Longitudinal resistance R as a function of moiré filling factor v and electric field E. b, Zoom-in phase diagram near half-band filling and zero E field.

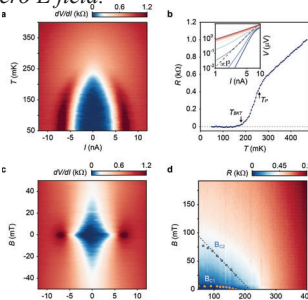


Figure 3: a, Differential resistance dV/dI as a function of current bias I and temperature T. b, Zero-bias resistance R as a function of T Insert: I-V characteristics at varying T c, Differential resistance dV/dI as a function of I and magnetic field B d, Zero-bias resistance R as a function of T and B.

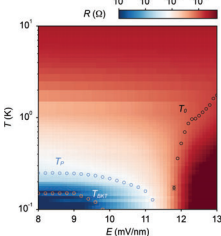


Figure 4: Zero-bias resistance R as a function of E and T, showing an electric-field-induced superconductor-insulator transition at v=1.

Figure 3 further investigates the differential conductance of the zero-resistance phase under applied perpendicular magnetic fields at elevated temperature. Figure 3a shows the differential resistance dV/dI as a function of bias current I and temperature T. The critical current is I_c=5 nA at T=50 mK and gradually decreased to zero near 250 mK. The corresponding zero-bias resistance R as a function of T is shown in Figure 3b, revealing

a Berezinskii–Kosterlitz–Thouless (BKT) transition temperature T_{p} =180 mK and a pairing temperature T_{p} =250 mK. Figure 3c shows dV/dI as a function of I and magnetic field B. Figure 3d shows zero-bias resistance R as a function of B and T, from which the critical fields B_{c1} and B_{c2} are identified.

A linear fit to
$$B_{c2} = \frac{\Phi_0}{2 \pi \xi^2} \left(1 - \frac{T}{T_p} \right)$$

shown as the dashed line, gives rise to a superconducting coherence length $\xi \approx 52$ nm, which is about 10 times the moiré period $a_M \approx 5$ nm (Φ_0 denotes the magnetic flux quantum).

Figure 4 shows R as a function of E and T, revealing an electric-field-induced superconductor-insulator transition at v=1. The critical temperatures $T_{\rm BKT}$ and $T_{\rm p}$ are indicated on the superconducting side and the extracted thermal activation gaps $T_{\rm o}$ are plotted on the insulating side. All characteristic temperature scales vanish continuously as E approaches the critical field $E_{\rm c}{\approx}11.7~{\rm mV}$ / nm, indicating a continuous quantum phase transition.

Conclusions and Future Steps:

We observe robust superconductivity in tWSe₂, emerging at the verge of correlated insulating state at v=1. The continuous superconductor-insulating transition highlights the delicate interplay between the kinetic energy t and on-site interaction U, resembling the physics of high- T_c cuperate superconductors. A superconducting transition temperature to Fermi temperature ratio (T_c/T_f) of 1-2%, along with a short coherence length $\xi/a_M \approx 10$ (both comparable to values in cooperate superconductors), further suggest strong pairing. Our findings motivate further investigations into questions such as the superconducting pairing symmetry and underlying pairing mechanism.

References:

- [1] Tang, Y. et al. Nature 579, 353-358 (2020)
- [2] Regan, E. C. et al. Nature 579, 359-363 (2020)
- [3] Anderson, P. W. Science 235, 1196-1198 (1987)
- [4] Hubbard, J. Proc. R. Soc. A 276, 237-257 (1963)
- [5] Lee, P. A., Nagaosa, N., Wen, X.-G. Reviews of Modern Physics 84, 1383-1417 (2012)
- [6] Imada, M., Fujimori, A., Tokura, Y. Reviews of Modern Physics 70, 1039-1263 (1998)